

SUPPORTING INFORMATION

Highly Selective, Red Emitting BODIPY-Based Fluorescent Indicators for Intracellular Mg²⁺ Imaging

*Qitian Lin and Daniela Buccella**

Department of Chemistry, New York University, New York, New York 10003

Table of Contents

1. Supporting figures and schemes	2
2. Additional experimental details	8
2.1. General procedure for the preparation of quantitative solutions of MagQ1 and MagQ2	8
3. NMR spectroscopy and chromatographic data for new compounds	9

1. Supporting figures and schemes

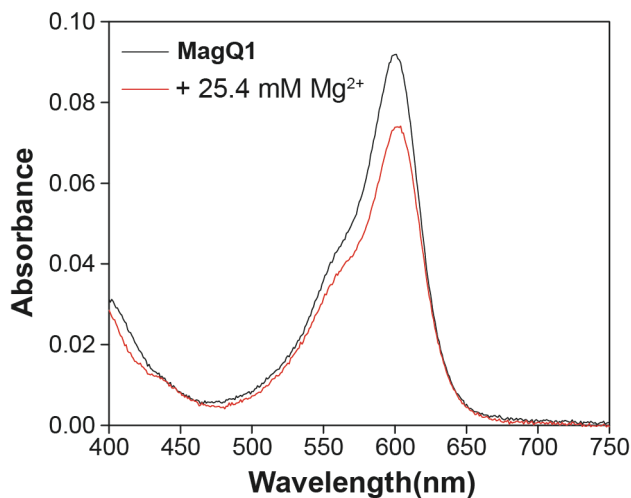


Figure S1. Absorption spectrum of **MagQ1** in 50 mM PIPES, 100 mM KCl, pH 7.0 buffer, 25 °C before (black line) and after (red line) treatment with Mg²⁺.

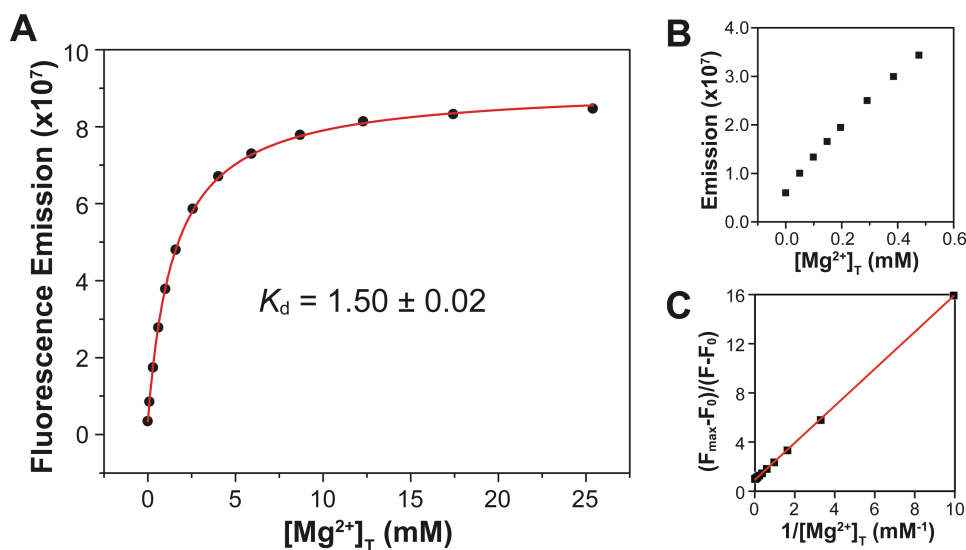
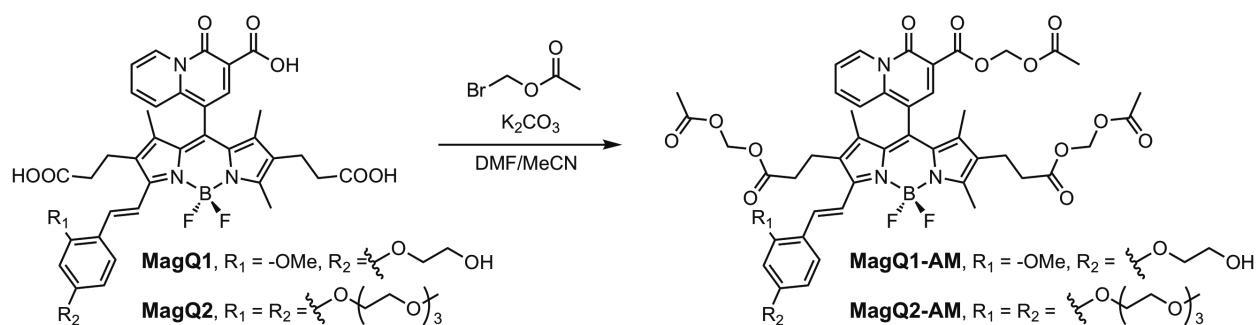


Figure S2. Fluorescence response of **MagQ1** to increasing concentrations of Mg²⁺ in 50 mM aqueous PIPES buffer, 100 mM KCl, pH 7.0, 25 °C. (A) Non-linear fit (red line) of the integrated fluorescence emission (black circles) as a function of total magnesium concentration, [Mg²⁺]_T, using a 1:1 metal-to-indicator binding model. (B) Integrated fluorescence emission as a function of total magnesium concentration, [Mg²⁺]_T, at low magnesium concentrations. (C) Benesi-Hildebrand plot.



Scheme S1. Synthesis of **MagQ1-AM** and **MagQ2-AM**.

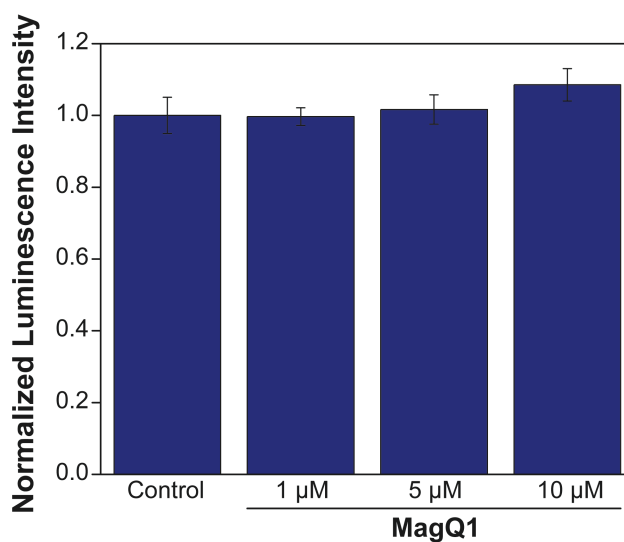


Figure S3. Viability of HeLa cells treated with **MagQ1** (in the membrane permeable acetoxymethyl ester form, **MagQ1-AM**) under typical sensor loading and imaging conditions, as determined by CellTiter-Glo® Luminescent Cell Viability Assay. Error bars correspond to standard deviations on eight replicas.

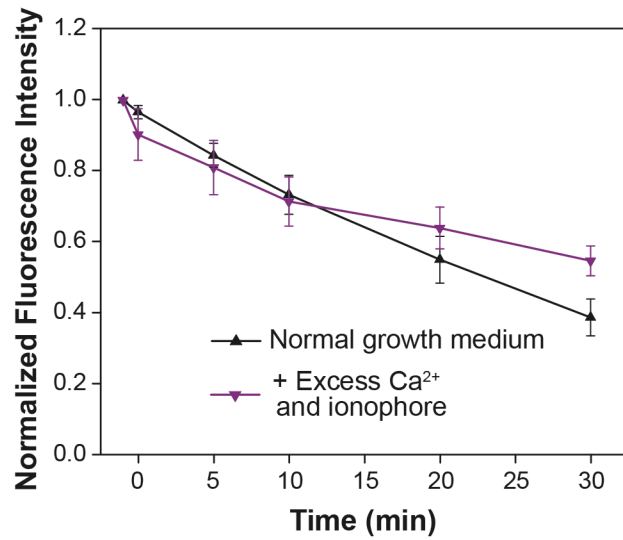


Figure S4. Normalized average fluorescence of **MagQ1** per cell in samples imaged in normal growth medium (black triangles) or under supplementation with exogenous Ca^{2+} and ionophore (violet triangles). Error bars represent the SD, $N = 20$ cells.

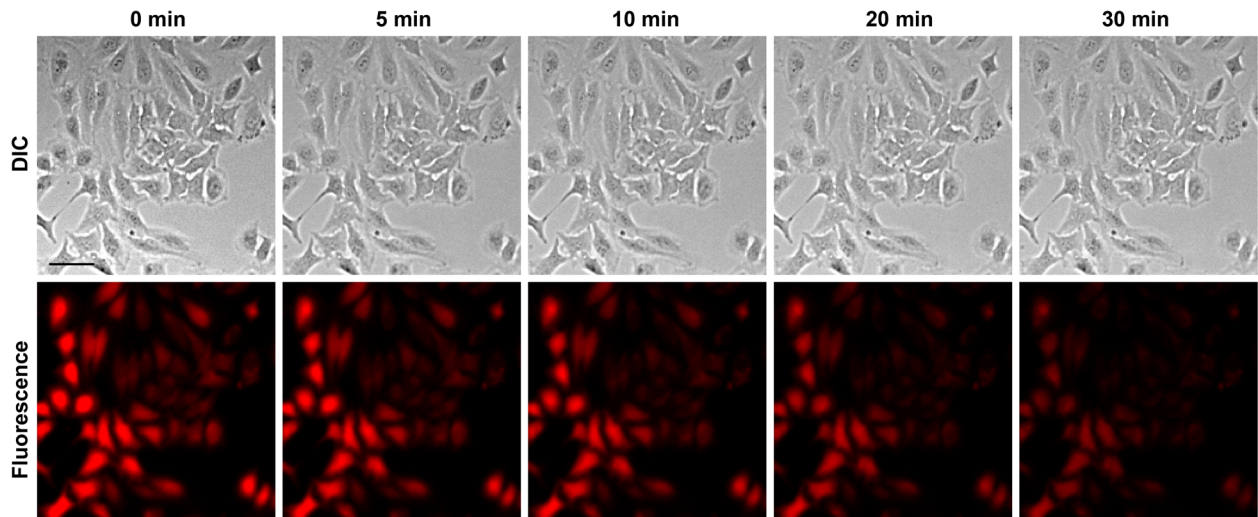


Figure S5. Fluorescence imaging of Mg^{2+} in live HeLa cells loaded with **MagQ1-AM** over a period of 30 min. Cells incubated in HHBSS, containing 0.8 mM Mg^{2+} , and 1.8 mM Ca^{2+} . Scale bar: 50 μm .

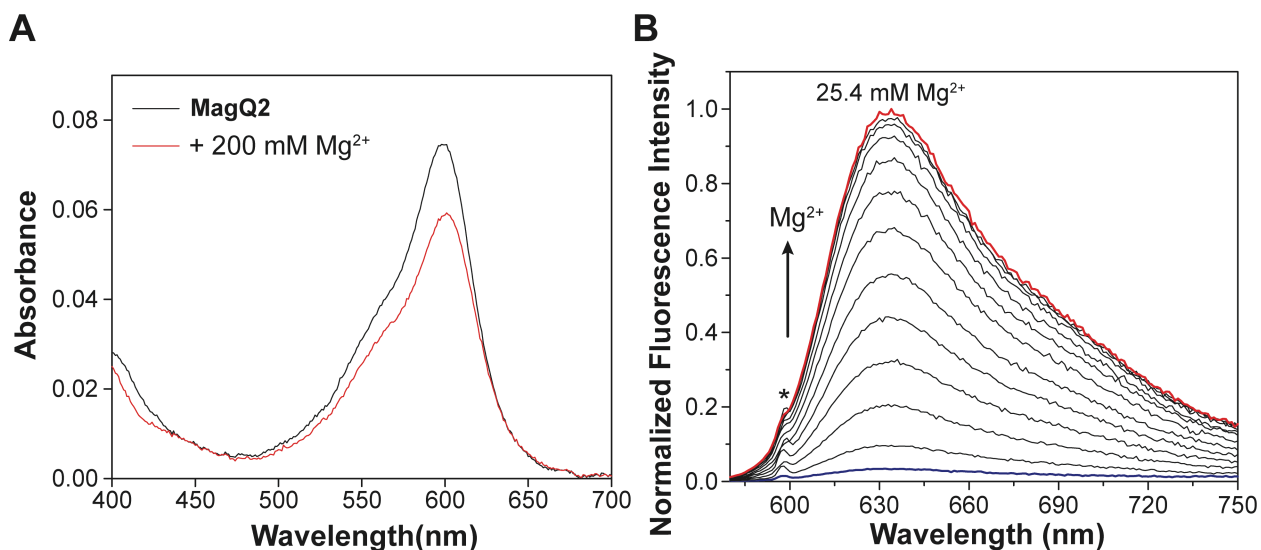


Figure S6. (A) Absorption and (B) fluorescence emission spectra of a 1.0 μM solution of **MagQ2** treated with increasing concentrations of Mg^{2+} . Titration conducted in 50 mM aqueous PIPES buffer, 100 mM KCl, pH 7.0, 25 $^{\circ}\text{C}$. Excitation wavelength $\lambda_{\text{ex}} = 600 \text{ nm}$. * = scattered light from excitation beam.

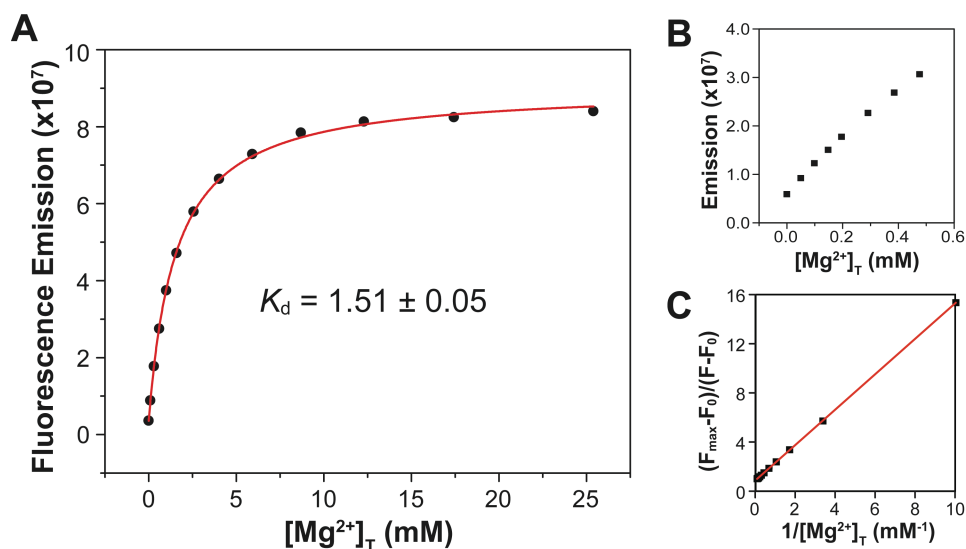


Figure S7. Fluorescence response of **MagQ2** to increasing concentrations of Mg^{2+} in 50 mM aqueous PIPES buffer, 100 mM KCl, pH 7.0, 25 $^{\circ}\text{C}$. (A) Non-linear fit (red line) of the integrated fluorescence emission (black circles) as a function of total magnesium concentration, $[\text{Mg}^{2+}]_{\text{T}}$, using a 1:1 metal-to-indicator binding model. (B) Integrated fluorescence emission as a function of total magnesium concentration, $[\text{Mg}^{2+}]_{\text{T}}$, at low magnesium concentrations. (C) Benesi-Hildebrand plot.

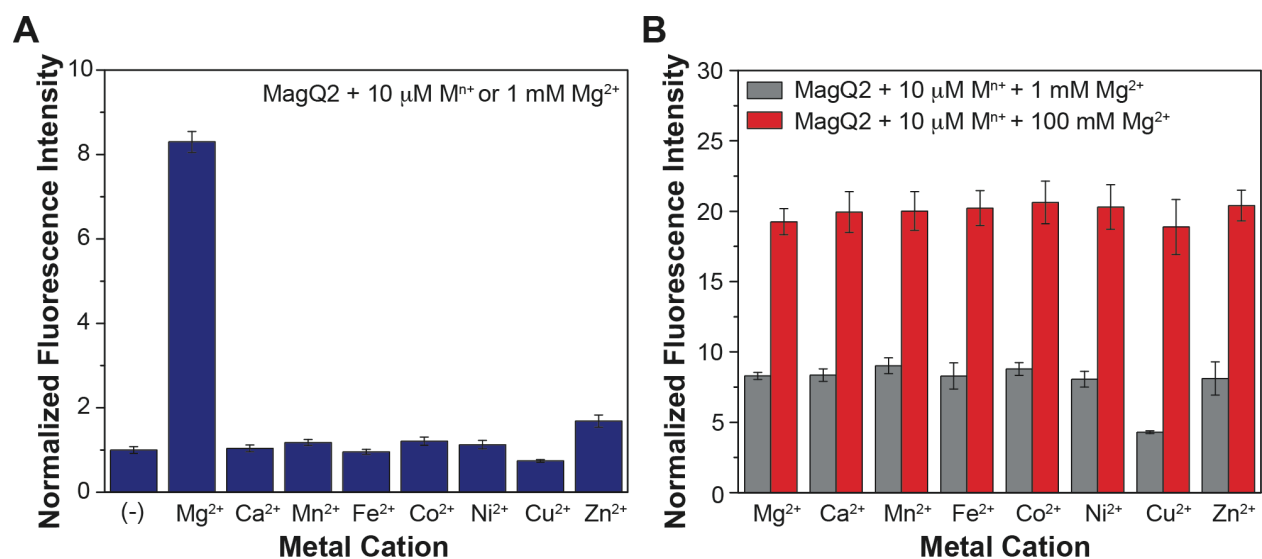


Figure S8. (A) Fluorescence response of 1 μM **MagQ2** to physiological concentration of Mg^{2+} (1 mM) or to other divalent metal ions (10 μM) in aqueous buffer at 25 $^{\circ}\text{C}$. (B) Fluorescence response of 1.0 μM **MagQ2** to 1 mM or 100 mM of Mg^{2+} in the presence of competing divalent cations, showing the selectivity of the detection in 50 mM PIPES, 100 mM KCl, pH 7.0 buffer. Error bars correspond to standard deviations on measurements conducted in triplicate.

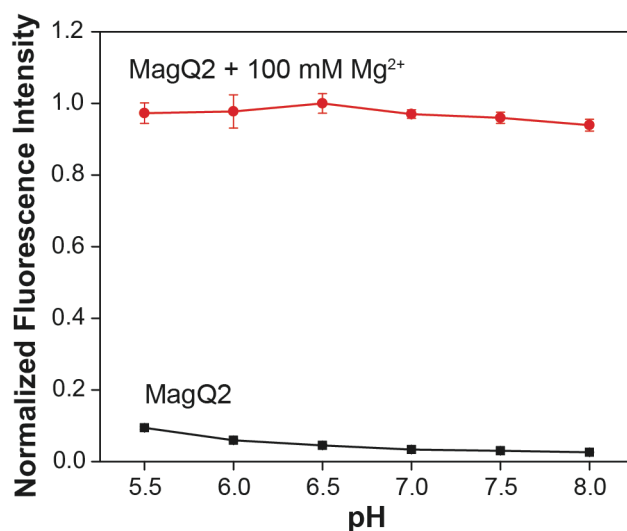


Figure S9. Fluorescence emission of a 1 μM solution of **MagQ2** in aqueous buffer at pH ranging from 5.5 to 8.0, 25 $^{\circ}\text{C}$, in the absence (black squares) or presence (red circles) of 100 mM Mg^{2+} . Error bars correspond to standard deviations on measurements conducted in triplicate.

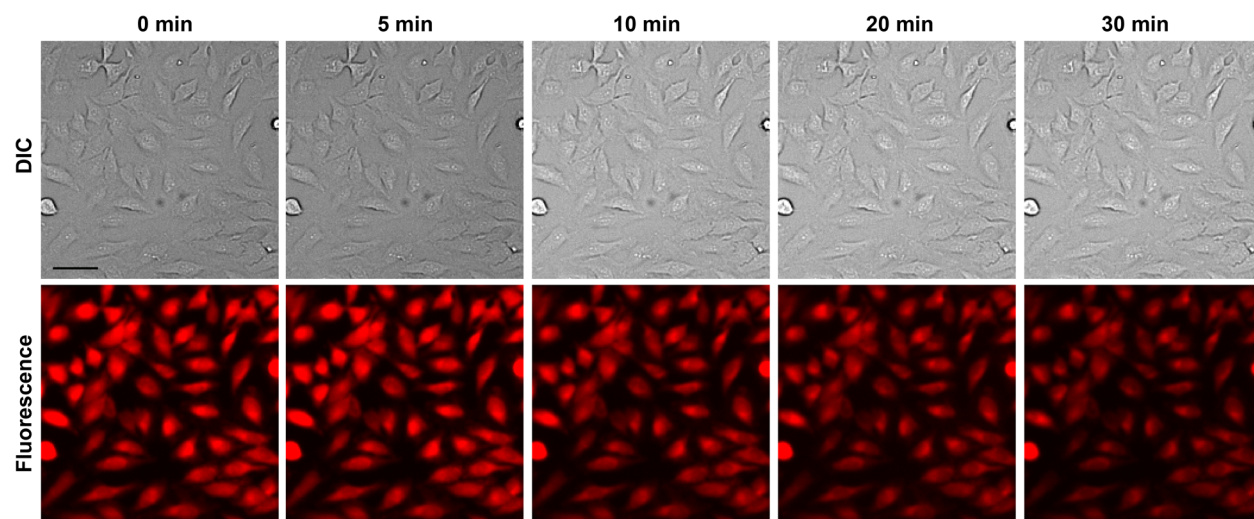


Figure S10. Fluorescence imaging of Mg^{2+} in live HeLa cells loaded with **MagQ2-AM** over a period of 30 min. Cells incubated in HHBSS, containing 0.8 mM Mg^{2+} and 1.8 mM Ca^{2+} . Scale bar: 50 μm .

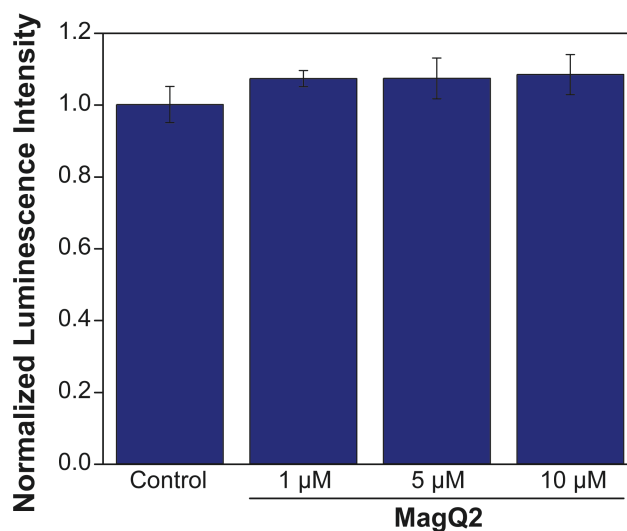


Figure S11. Viability of HeLa cells treated with **MagQ2** (in the membrane permeable acetoxymethyl ester form, **MagQ2-AM**) under typical sensor loading and imaging conditions, as determined by CellTiter-Glo® Luminescent Cell Viability Assay. Error bars correspond to standard deviations on eight replicas.

2. Additional experimental details

2.1. General procedure for the preparation of quantitative solutions of MagQ1 and MagQ2

A quantitative sample of **MagQ1** was weighed and dissolved in DMSO to prepare a 1.0 mM stock solution in a volumetric flask. The solution was divided into small aliquots, flash frozen in liquid nitrogen and stored at -20 °C until use.

An aliquot of the stock solution was diluted in aqueous buffer (50 mM PIPES, 100 mM KCl, pH 7.0) to obtain a series of solutions with concentrations ranging from 0.2 to 1.0 μM that were used to determine the molar absorptivity at 600 nm, 25 °C ($\epsilon = 84000 \pm 1000 \text{ M}^{-1}\cdot\text{cm}^{-1}$). This molar absorptivity was used in subsequent experiments to quantify the concentrations of **MagQ1** and **MagQ2** in various samples and stock solutions.

3. NMR spectroscopy and chromatographic data for new compounds

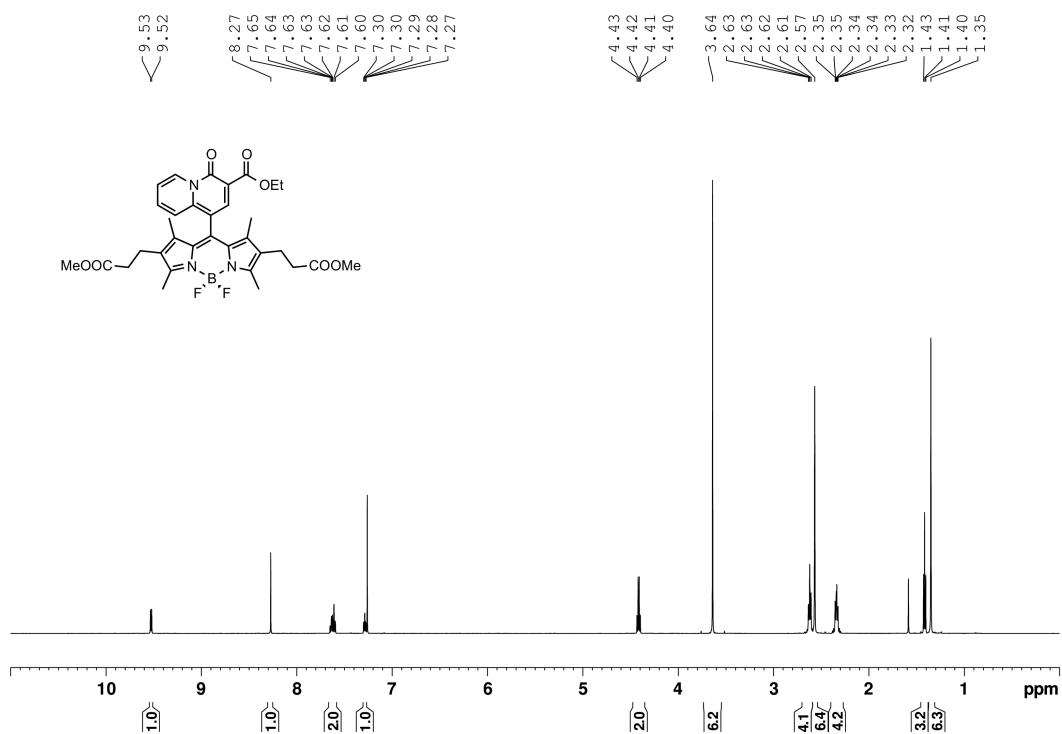


Figure S12. ¹H NMR spectrum of **3** in CDCl₃

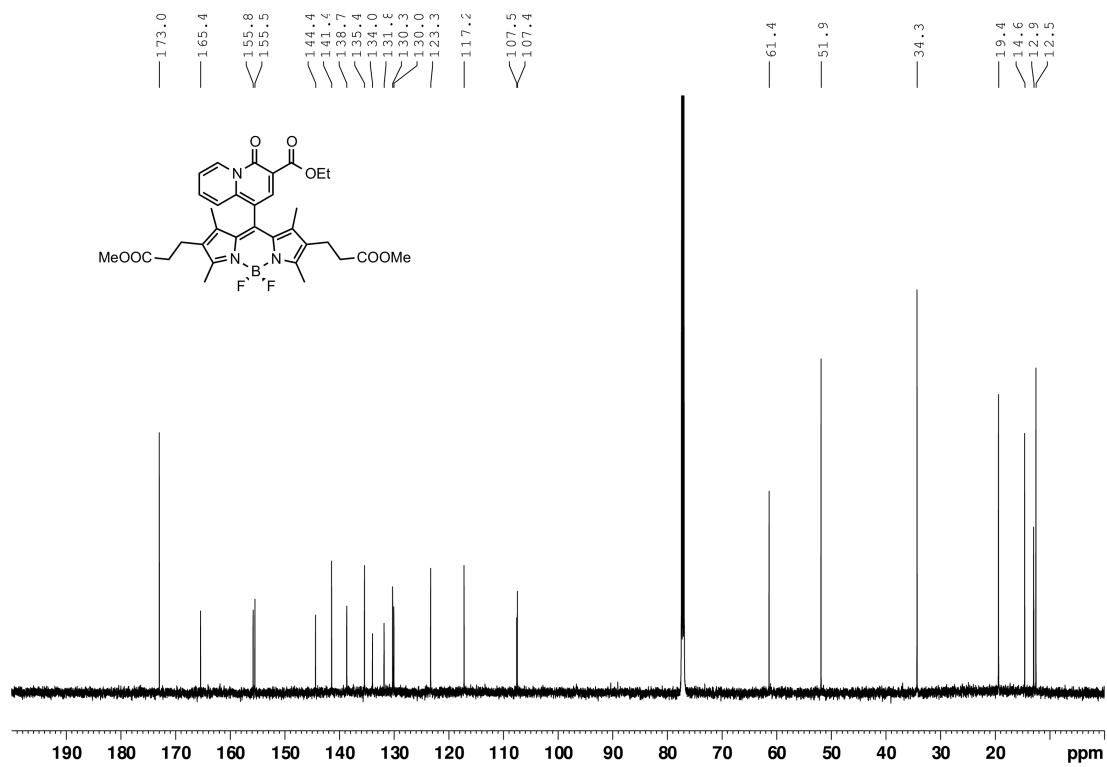


Figure S13. ¹³C{¹H} NMR spectrum of **3** in CDCl₃

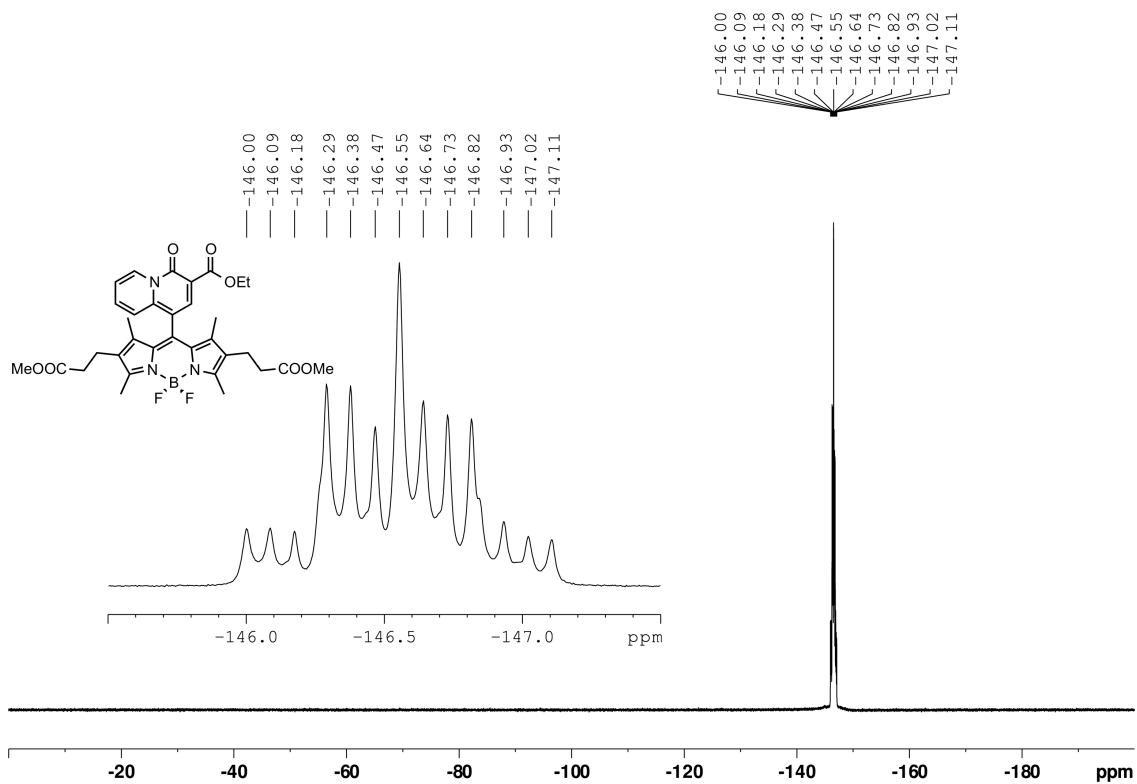


Figure S14. ¹⁹F NMR spectrum of **3** in CDCl₃

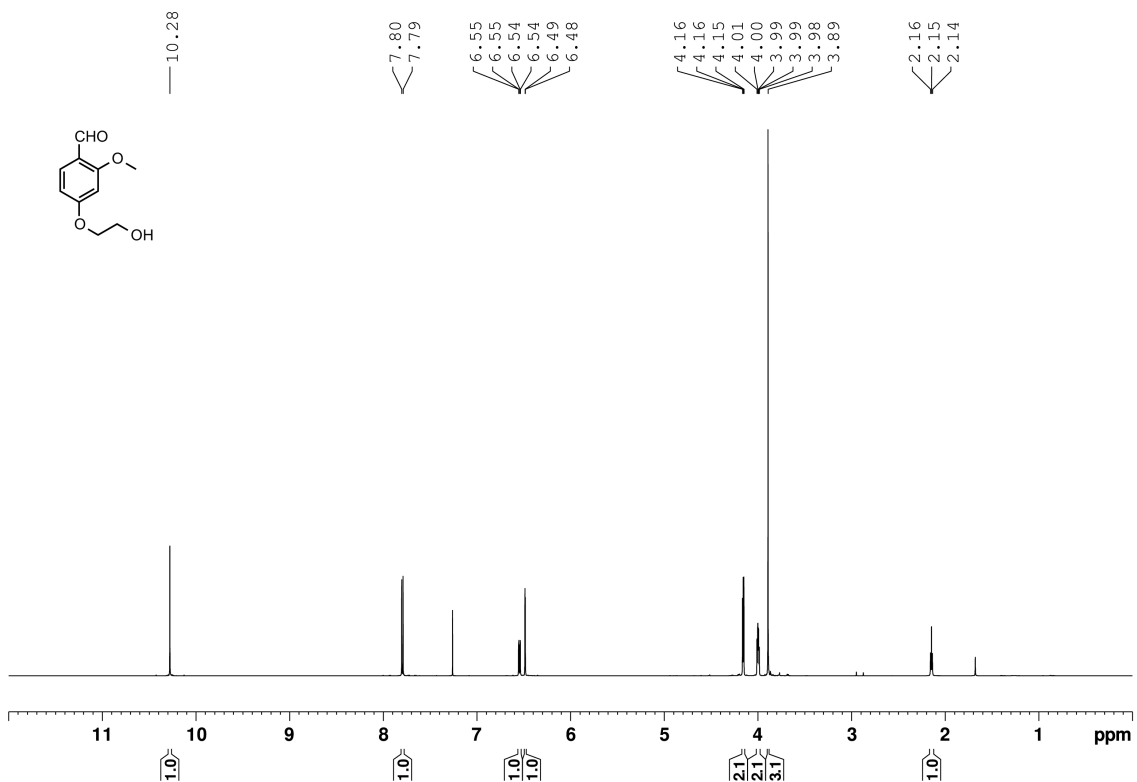


Figure S15. ¹H NMR spectrum of **4** in CDCl₃

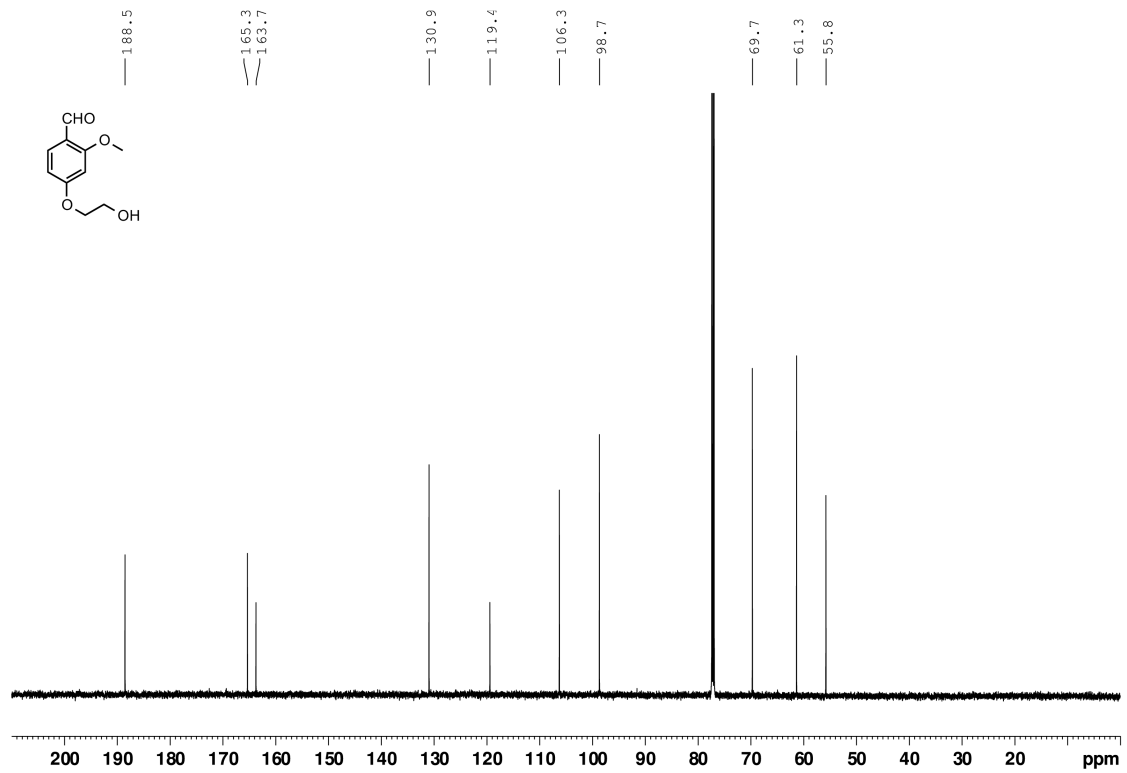


Figure S16. $^{13}\text{C}\{^1\text{H}\}$ NMR spectrum of **4** in CDCl_3

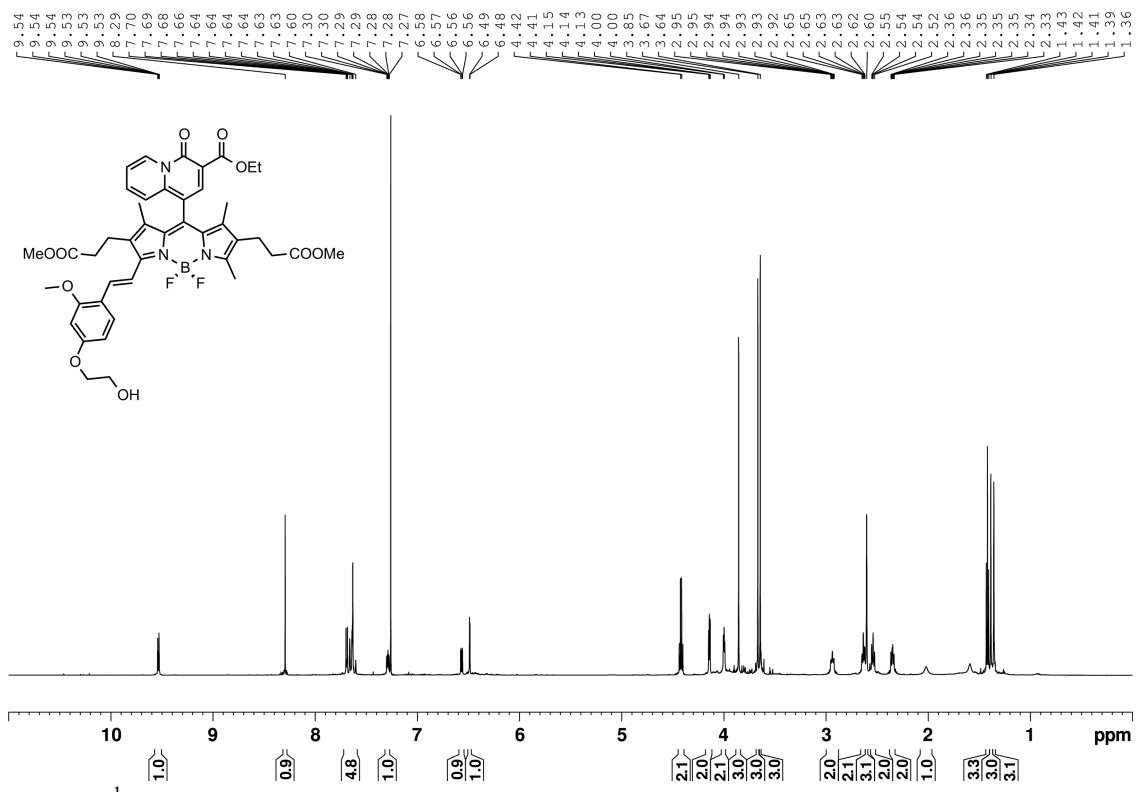


Figure S17. ^1H NMR spectrum of **6** in CDCl_3

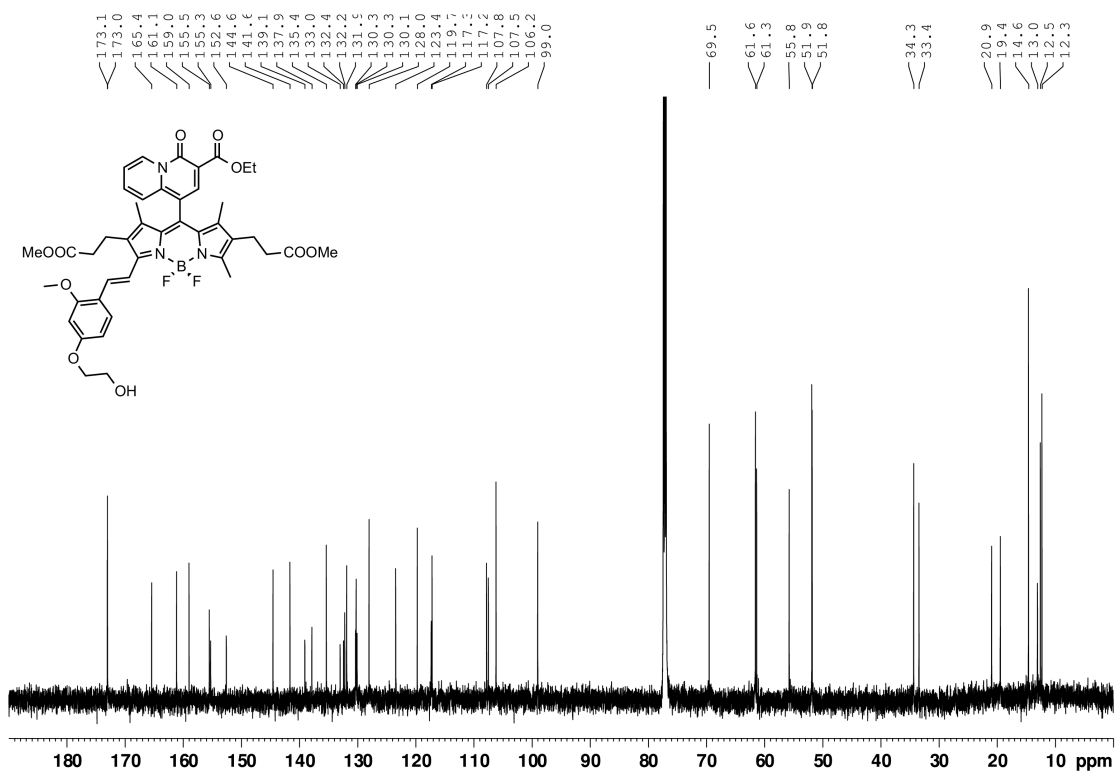


Figure S18. $^{13}\text{C}\{^1\text{H}\}$ NMR spectrum of 6 in CDCl_3

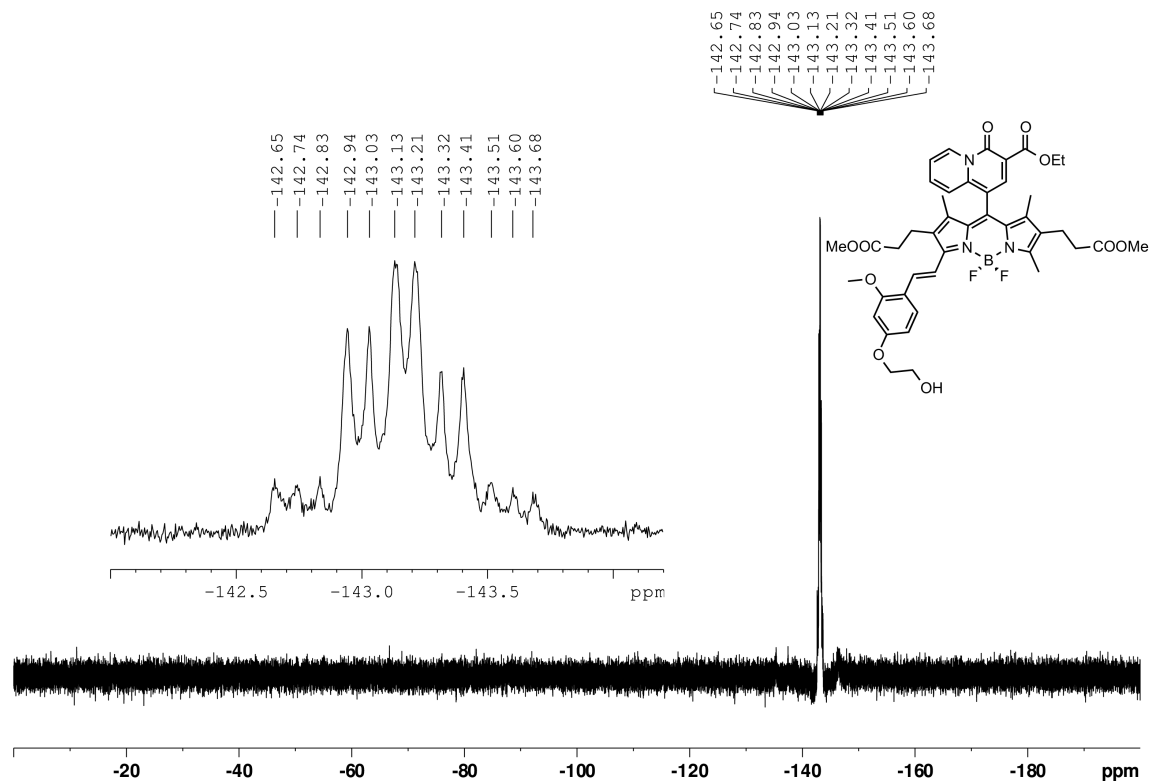


Figure S19. ^{19}F NMR spectrum of 6 in CDCl_3

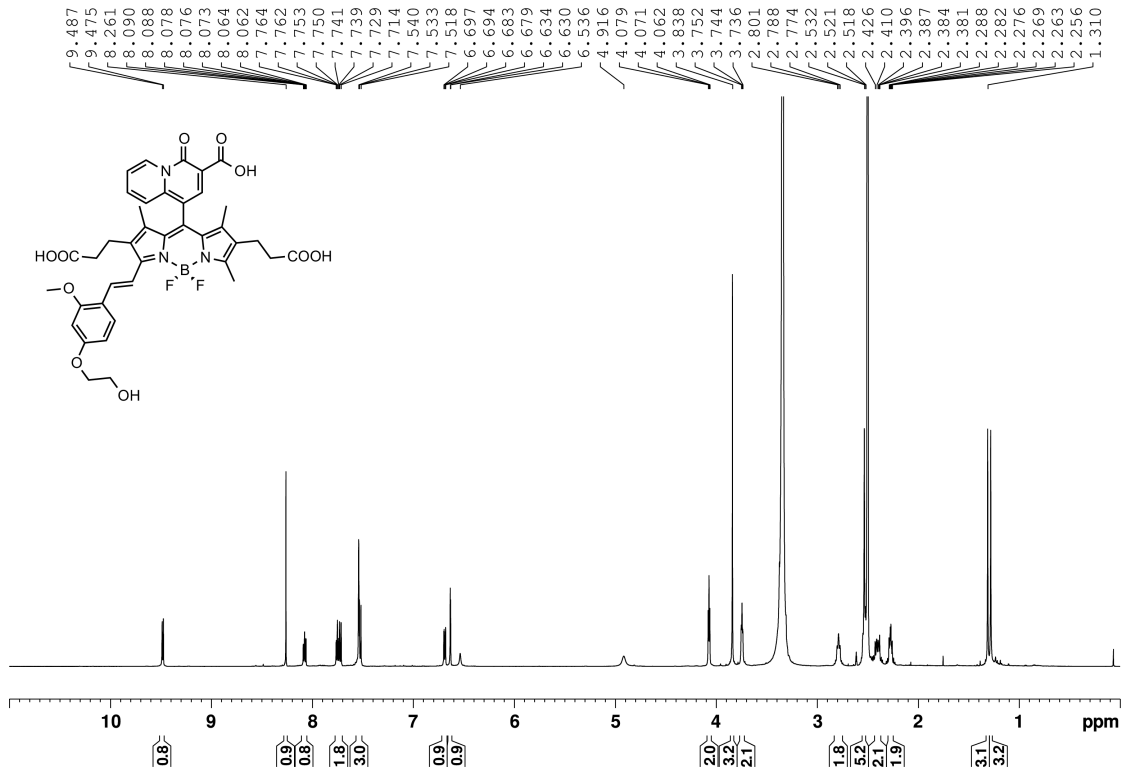


Figure S20. ¹H NMR spectrum of **MagQ1** in DMSO-d₆

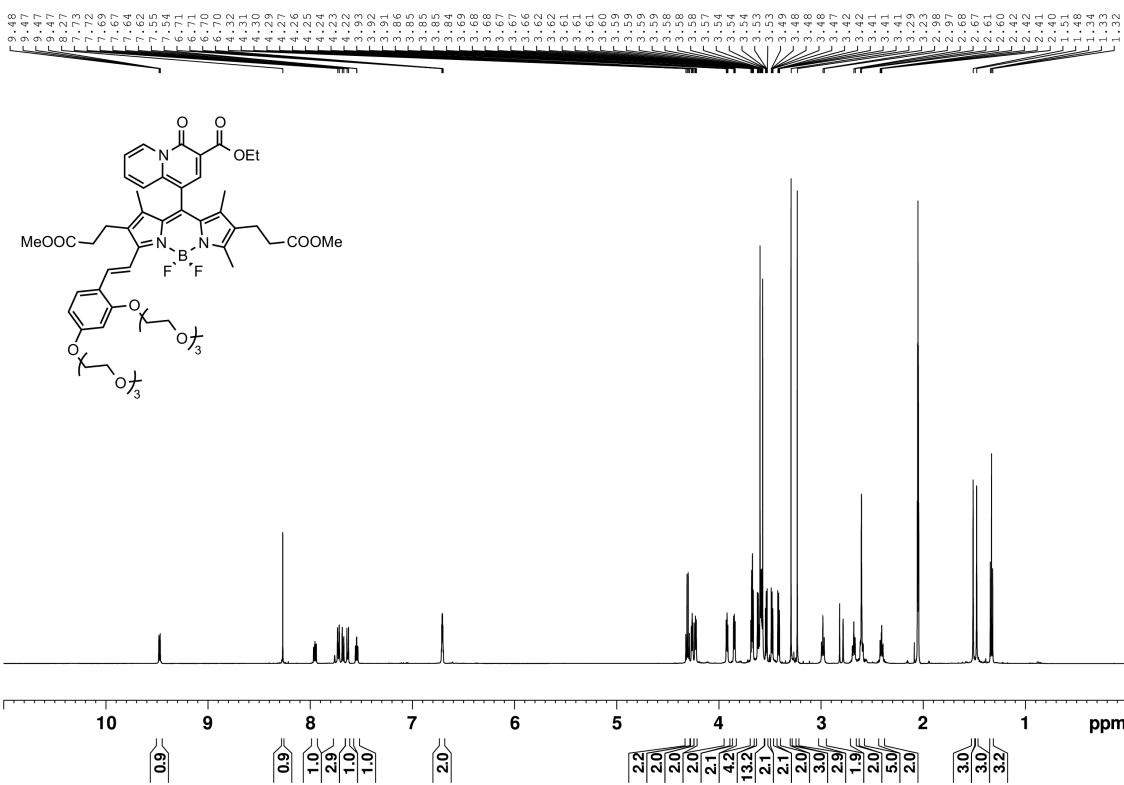


Figure S21. ¹H NMR spectrum of **7** in acetone-d₆

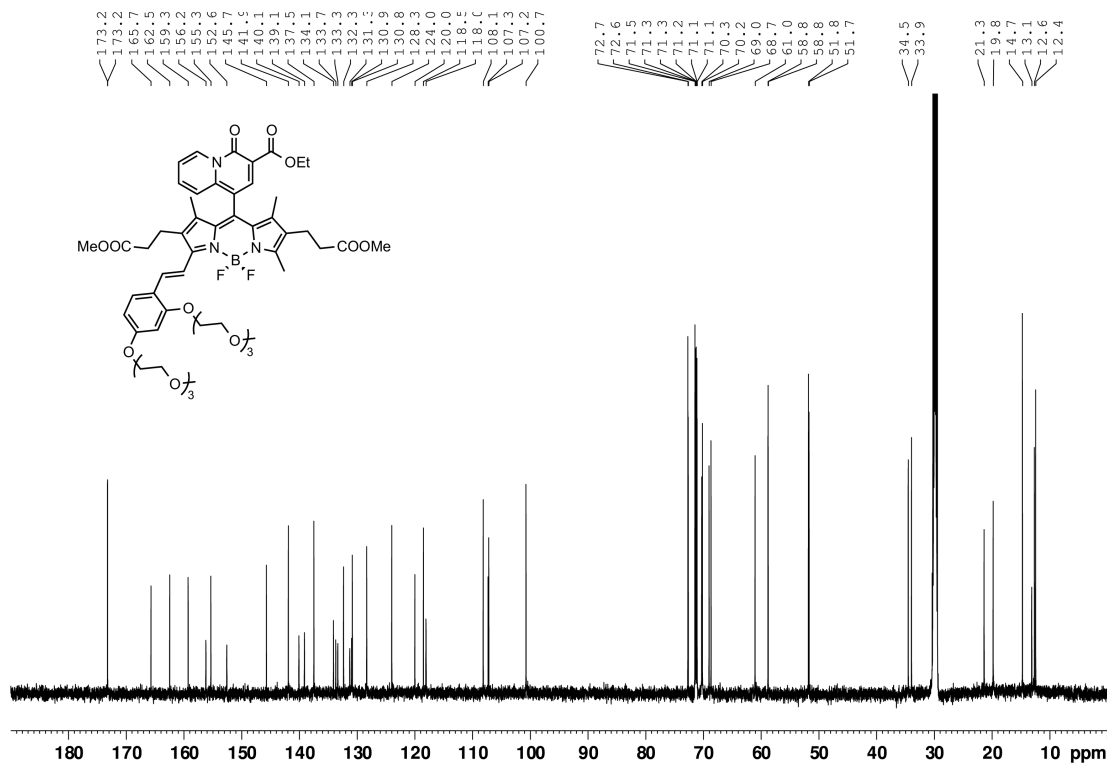


Figure S22. $^{13}\text{C}\{^1\text{H}\}$ NMR spectrum of 7 in acetone- d_6

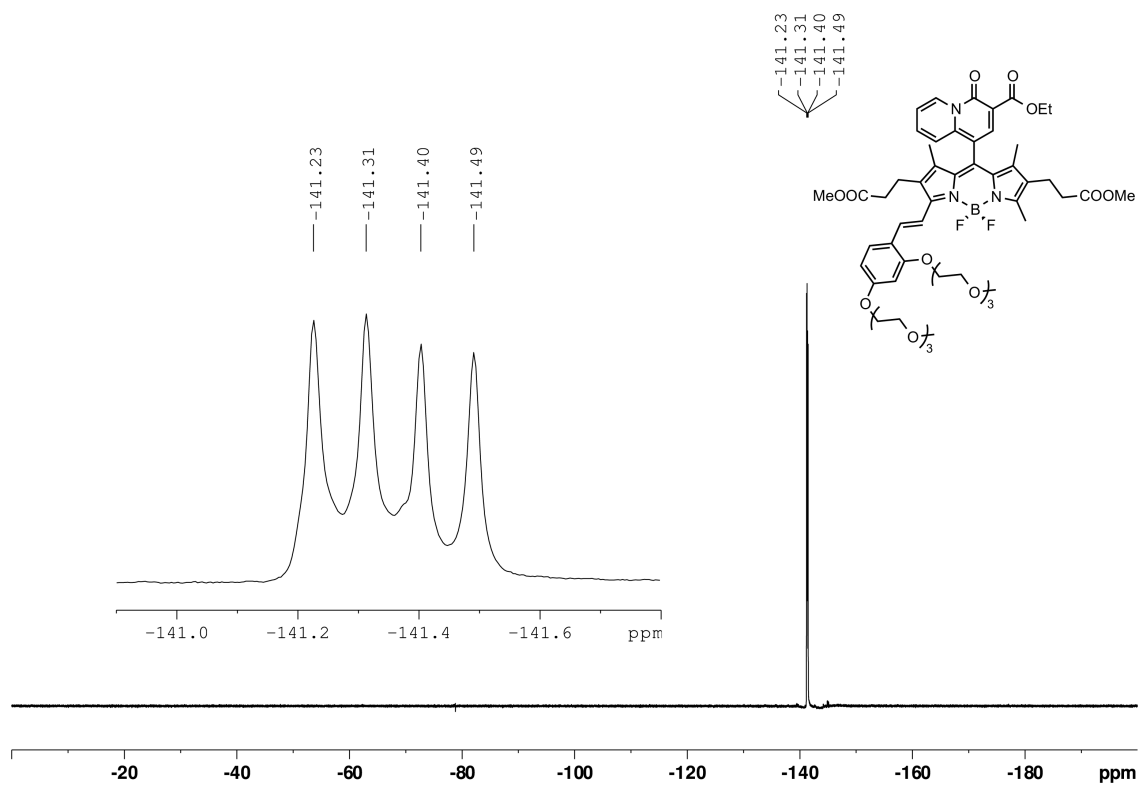


Figure S23. ^{19}F NMR spectrum of 7 in acetone- d_6

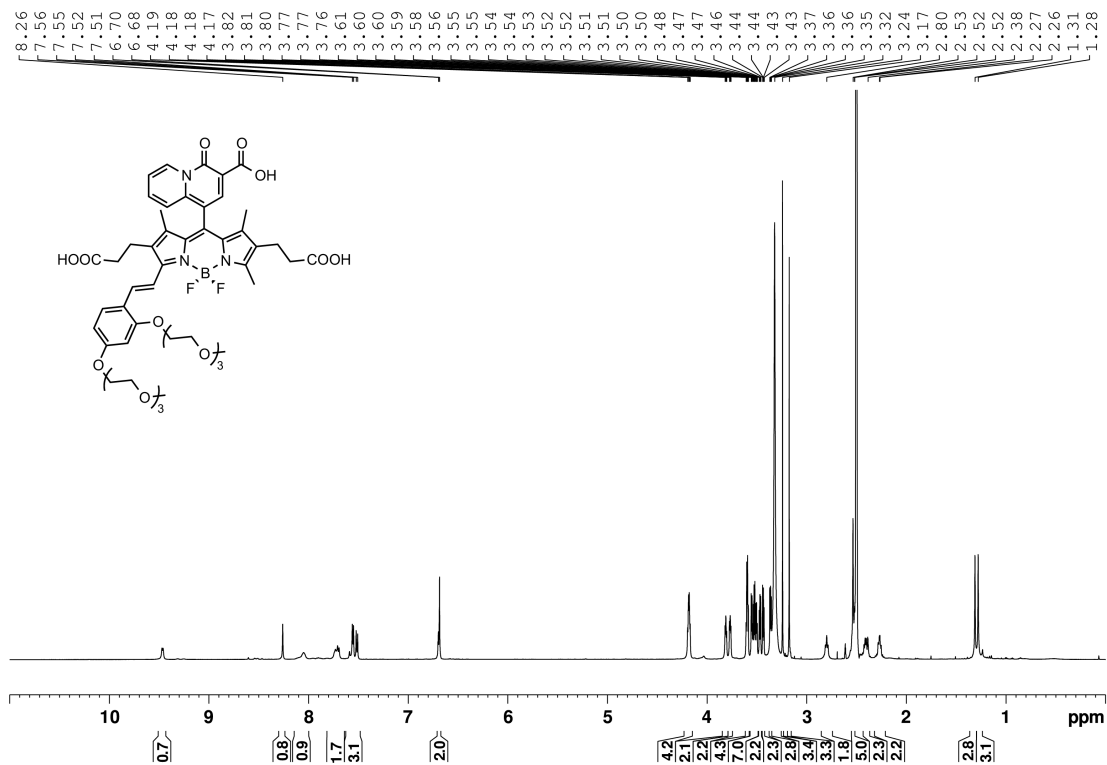


Figure S24. ^1H NMR spectrum of **MagQ2** in DMSO-d_6

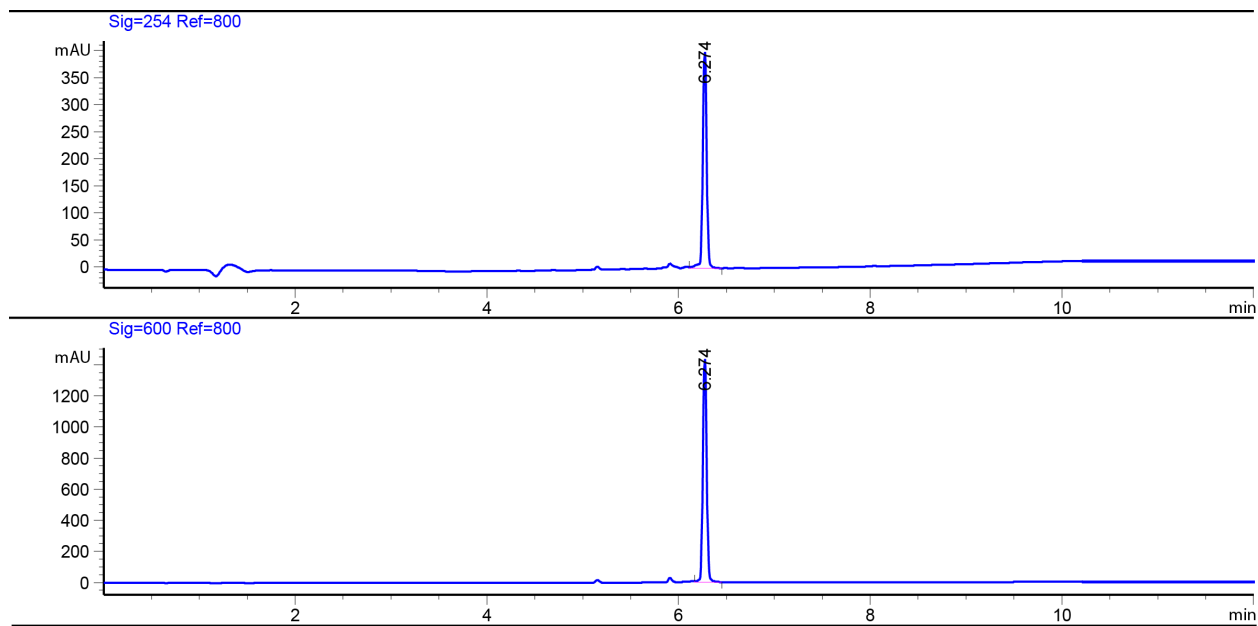


Figure S25. Reversed phase HPLC chromatogram of **MagQ1**, eluted with an acetonitrile/water (+0.1% TFA) gradient.

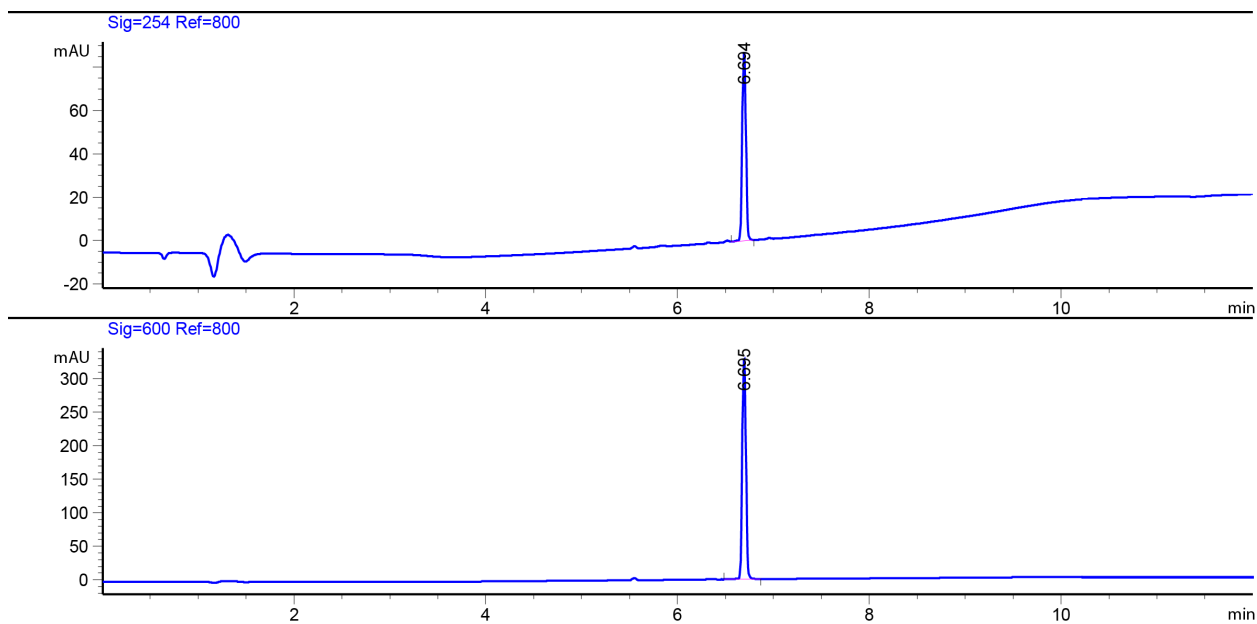


Figure S26. Reversed phase HPLC chromatogram of **MagQ2**, eluted with an acetonitrile/water (+0.1% TFA) gradient.

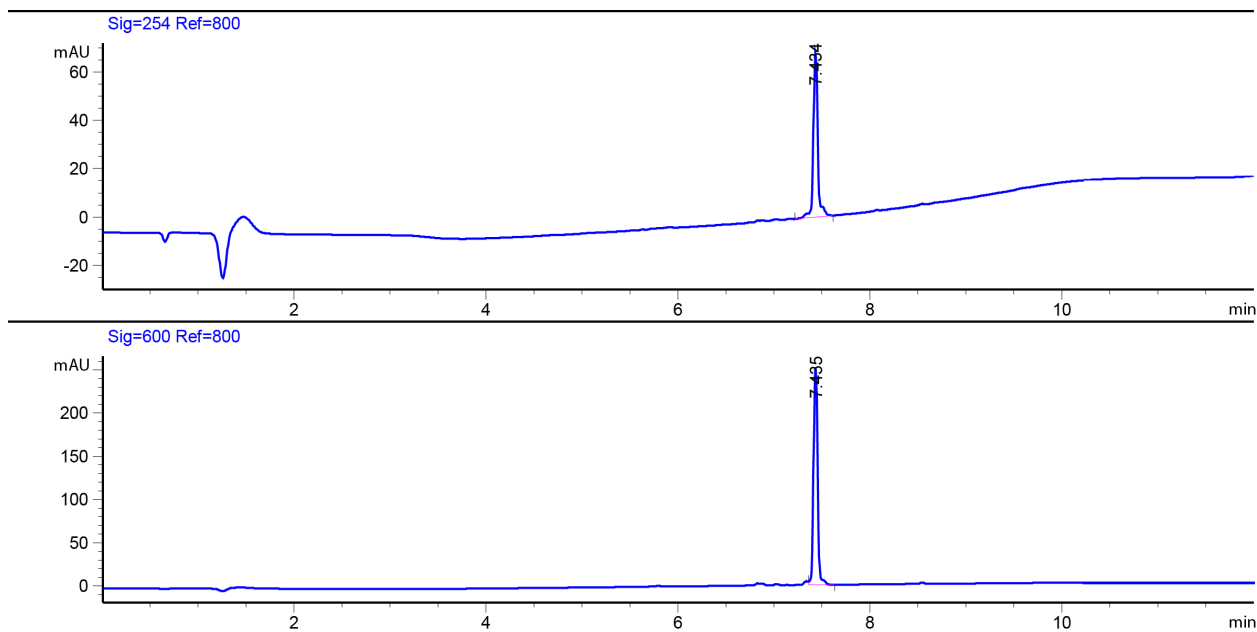


Figure S27. Reversed phase HPLC chromatogram of **MagQ1-AM**, eluted with an acetonitrile/water (+0.1% TFA) gradient.

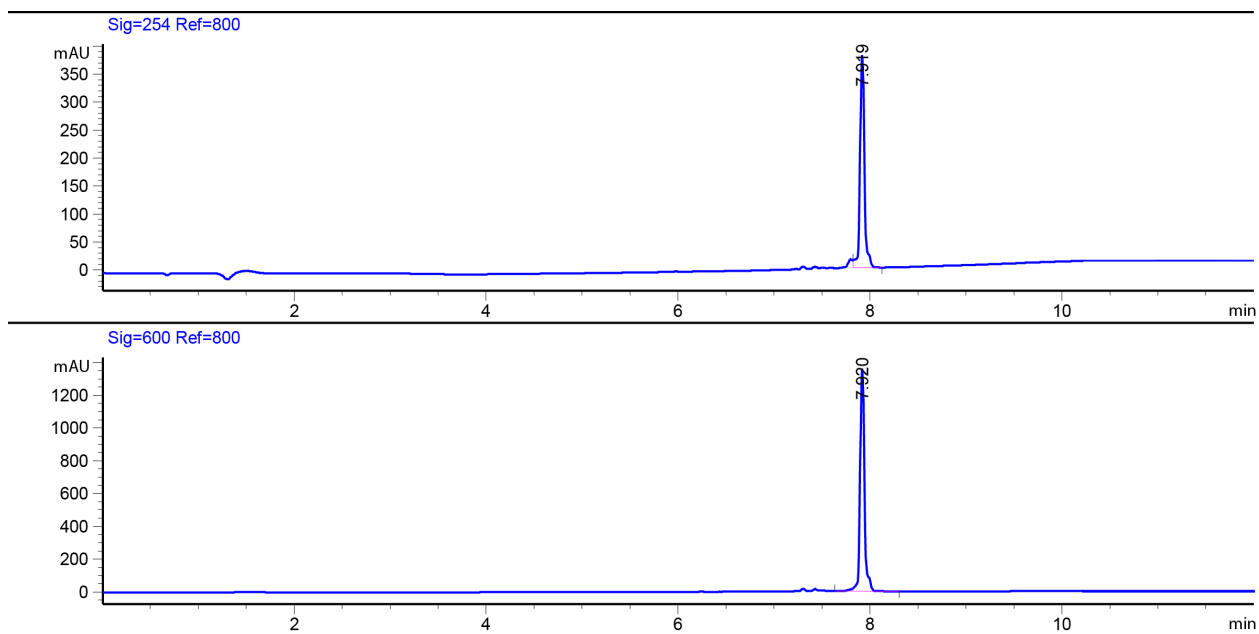


Figure S28. Reversed phase HPLC chromatogram of **MagQ2-AM**, eluted with an acetonitrile/water (+0.1% TFA) gradient.